[15]G. E. H. Reuter and E. H. Sondheimer, Proc. Roy. Soc. (London) A195, 336 (1948).
[16]The calculations were done on the Rutgers Bubble Chamber Group's PDP-6 computer which is supported in part by the National Science Foundation.
[17]G. L. Dunifer, thesis (University of California, 1968) (unpublished).
[18]R. Chui, R. Orbach, and B. L. Gehman, Phys. Rev. B 2, 2298 (1970).
[19]S. Schultz (private communication).
[20]Above 20°K phonon relaxation rapidly increases $1/\gamma T_{sl}$ and strong coupling again breaks down.
[21]J. A. Cameron, I. A. Campbell, J. P. Compton, R. A. G. Lines, and G. V. H. Wilson, Phys. Letters 20, 569 (1966).
[22]R. T. Longo and J. H. Pifer, Bull. Am. Phys. Soc. 15, 95 (1970).
[23]R. T. Longo and J. H. Pifer (unpublished).

PHYSICAL REVIEW B VOLUME 4, NUMBER 11 1 DECEMBER 1971

Transmission of U^{235} Fission Fragments in Solid Media

V. Aiello,* G. Maracci, and F. Rustichelli†
Physics Division, Joint Research Center, Euratom, Ispra, Italy
(Received 6 April 1971)

Transmission measurements of the fission fragments arising in U^{235} thermal-neutron-induced fission were performed in Mg, Al, Fe, and Ag by using a back-to-back fission chamber. From the transmission curves, it is possible to derive the relative atomic stopping powers of the different targets and the ranges of the fission fragments in the elements investigated. The experimental results are compared with the theoretical calculations of Lindhard, Scharff, and Schiøtt concerning the loss of energy of heavy ions in matter.

INTRODUCTION

Much experimental information is available concerning the energy loss of charged particles in matter. The parameters which are varied from experiment to experiment are the mass numbers, the atomic numbers, the electrical charges and the energies of the incident particles, and the mass numbers and the atomic numbers of the stopping materials.

Lindhard, Scharff, and Schiøtt (LSS)[1] have developed a general theory for the energy loss of heavy ions in matter, using a Thomas-Fermi statistical model for interacting atoms to predict both electronic and nuclear stopping powers. Their theory, which does not contain adjustable parameters, resulted in agreement with a wide class of different experiments[1] previously performed. Most of the subsequent experimental results[2–31] were compared with the LSS theory, which generally appears to be able to explain the fundamental mechanism of the loss of energy of charged particles.

However, there are several cases in which the theory shows some discrepancies from the experimental values. For instance, an oscillatory dependence of the electronic stopping cross section on the atomic number Z_1 of the projectile was observed[9] for Al and C. Also, an oscillatory dependence on the atomic number Z_2 of the stopping element was observed[29] by using α particles as projectiles. This behavior is not foreseen by the unmodified LSS theory, which gives a monotonic dependence of the stopping cross section on both Z_1 and Z_2.

The present experiment consists of transmission measurements on the fission fragments arising in U^{235} thermal-neutron-induced fission. The stopping elements Mg, Al, Fe, and Ag were used. From the transmission curves it is possible to derive the relative atomic stopping powers of the different target elements and the corresponding ranges. The aim of the experiment was to add new data to those existing in the field of energy loss of U^{235} fission fragments and to test the LSS theory for the dependence of the stopping power for fission fragments on the atomic number Z_2 of the stopping element.

EXPERIMENTAL METHOD

The method utilized is practically the same as that of Segrè and Wiegand.[32] The measurements were carried out by irradiating a back-to-back fission chamber (Fig. 1) in the thermal column of the RB-2 reactor of Montecuccolino (Bologna). The double fission chamber[33] is a gas flow counter utilizing argon containing 2% nitrogen. The electrode spacing was 10 mm and the gas pressure was adjusted slightly above ambient pressure. The operating voltage was 500 V positive applied to each anode. The fission-fragment source was a thin deposit of natural uranium, with a thickness of 0.2 mg/cm^2 and a diameter of 12 mm, obtained by vacuum evaporation on a Pt disc of 0.1-mm thickness and 20-mm diameter. The amount of fissionable material was determined with an ac-

curacy of 0.8% by combining chemical analysis and x-ray intercalibration.[33]

The natural uranium deposit was positioned in one of the two ionization chambers, constituting the back-to-back counter, which was irradiated in a thermal neutron flux of ~ 10^9 n/cm^2 sec. During the irradiation, one detected the fission fragments transmitted through a thin sheet of the element under investigation which was positioned directly on the uranium deposit. The thickness of the sheet was varied from measurement to measurement.

A second uranium deposit positioned on the other ionization chamber acted as a monitor for the neutron flux in the different irradiations. In particular, it was utilized in order to eliminate from the fission counting rate of the first deposit the background pulses having a height above the discriminator setting. These spurious pulses are produced by interaction of neutrons with fissile impurities existing in the counter walls, and their number is proportional to the neutron flux.[34] The experimental correction was effected by performing an irradiation with the second uranium deposit used to normalize the neutron flux and with a Pt disc without uranium deposit in the first chamber. The experimental arrangement is shown schematically in Fig. 1.

The bias setting was at an energy of ~ 13 MeV in order to discriminate for background due to α particles, γ rays, or electronic noise. The deposits of Mg, Al, Fe, and Ag were obtained by lamination or by vacuum evaporation on glasses and subsequent removal from the substrate. The purity of Mg samples was better than 99.8%, of Al samples better than 99.5%, of Fe samples better than 99.5%, and of Ag samples better than 99.8%.

A rough check of the thickness homogeneity of the targets was performed by cutting the stopping element foils into pieces having the same surface of 25 mm^2 and comparing the weights. Relative deviations lower than 5% were found for Mg, Al, and Ag, and lower than 10% for Fe. The reported errors in the experimental data take into account mainly the uncertainties associated with the lack of perfect purity of the stopping elements, the thickness inhomogeneities, the counting statistics, and the corrections for background.

RESULTS

The experimental curves obtained for Mg, Al, Fe, and Ag are shown in Fig. 2. The uncertainties in the case of Fe are higher due to the difficulties in the preparation of thin samples. It appears that all the transmission curves have similar behavior apart from the quantitative difference in the stopping powers. This fact can be seen more clearly in Fig. 3 where the experimental points corresponding to each element were found to follow closely the experimental curve of Al when each abscissa was multiplied by a convenient factor. This factor represents the mass stopping power of the element considered relative to Al.

This close superposition shows that the behaviors of the transmission curves are independent of Z_2, despite the complicated distribution of atomic numbers and energies of the fission fragments. This fact was already observed by Segre and Wiegand, who measured transmission curves of U^{235} fission fragments in Al, Cu, Ag, Au, and collodion.

The mass stopping powers obtained for the different elements relative to Al are shown in Table I. Actually, due to the fact that the fission fragments are detected with a bias energy E_b, the transmission curves obtained cannot be used directly to derive absolute data concerning the energy loss. In fact, a fission fragment, having energy E and atomic number Z_1, which is stopped by the element with atomic number Z_2 and which has a range

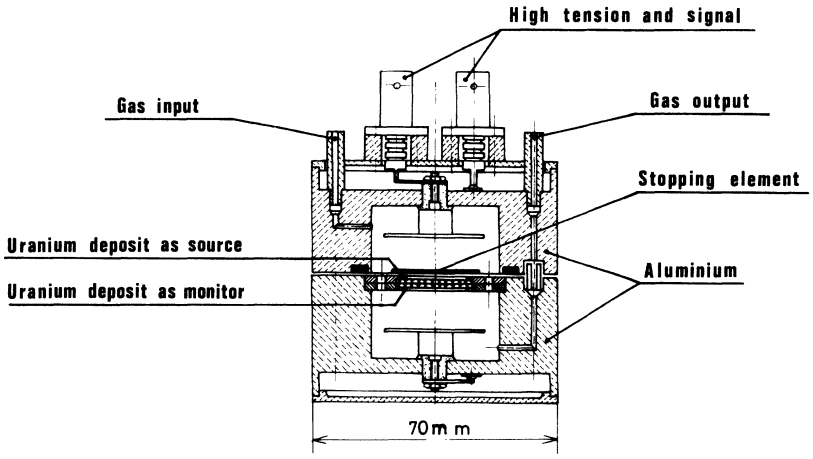

FIG. 1. Scheme of the experimental arrangement.

$$R_t\,(Z_1,\ Z_2,\ E)=\int_E^0 \frac{1}{dE/dX}\,dE \qquad (1)$$

is actually seen by the fission chamber as if it had the experimental range

$$R_e\,(Z_1,\ Z_2,\ E,\ E_b)=\int_E^{E_b} \frac{1}{dE/dX}\,dE \quad , \qquad (2)$$

where E_b is the bias energy of the counter.

However, Segrè and Wiegand found that by changing E_b the transmission curves of the various substances change, as expected, but the ratio between the effective stopping powers of the different elements stays practically constant. That is, by changing E_b all the transmission curves for different Z_2 remain the same if the abscissa scale of each curve is multiplied by a common factor. A discussion of this fact will be presented in Appendix B.

On this basis it is assumed that the relative stopping powers deduced from the transmission curves are the same that would be obtained with $E_b = 0$. Table I also contains the relative atomic stopping powers, which are obtained by dividing

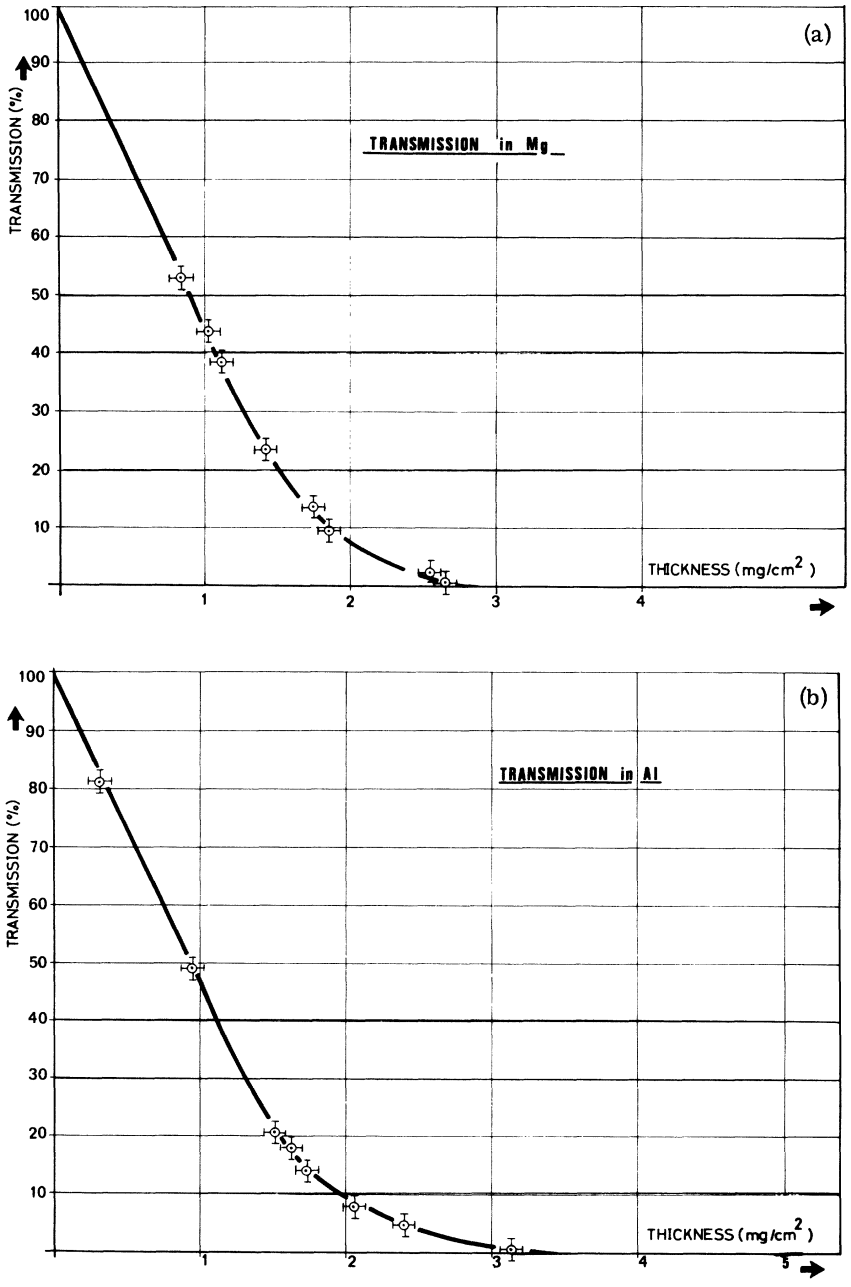

FIG. 2. Transmission curves of U^{235} fission fragments in Mg, Al, Fe, and Ag.

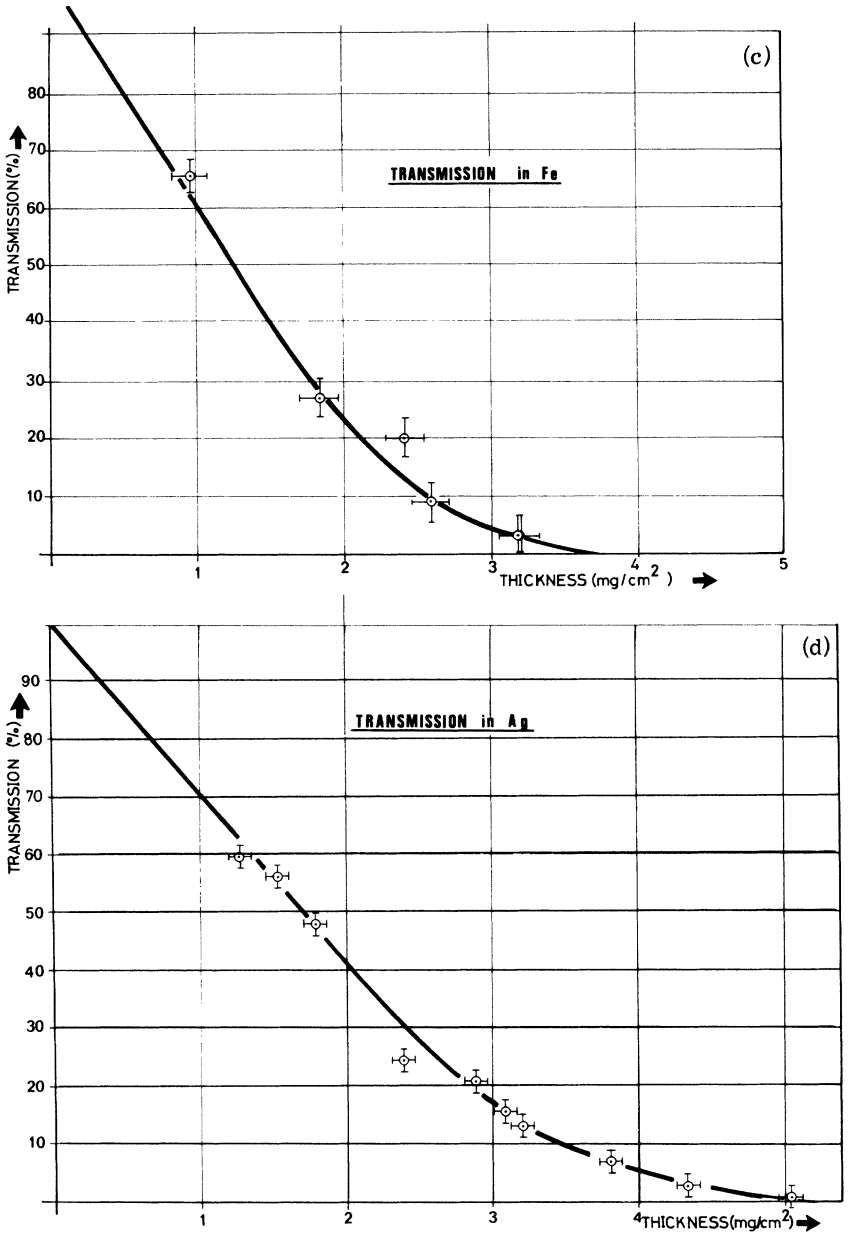

FIG. 2 (*Continued*).

the mass stopping powers by the number N of stopping atoms per cm^3.

In addition, Table I contains the ranges of U^{235} fission fragments in the different elements as obtained by combining the stopping powers relative to Al with the value of the absolute range in Al measured by Segrè and Wiegand[32] by an activation technique.

The stopping powers of the different elements relative to Al are given in Fig. 4 together with the results of the Segrè and Wiegand experiment.

DISCUSSION

The unified expression obtained by LSS for the electronic atomic stopping power is

$$-\frac{1}{N}\frac{dE}{dX} = \xi_e\, 8\pi\, e^2\, a_0\, \frac{Z_1 Z_2}{(Z_1^{2/3}+Z_2^{2/3})^{3/2}}\, \frac{v}{v_0}\,, \quad (3)$$

where a_0 and v_0 are the radius and velocity of the first Bohr orbit of hydrogen, v is the velocity of the projectile, N is the atomic density of the stopping material, e is the electronic charge, and ξ is a constant "of the order of $Z_1^{1/6}$."[1]

Northcliffe[35] has emphasized that since Eq. (3) is based on a Thomas-Fermi description of both projectile and stopping material, its applicability is limited to $Z_1 > 10$ and $Z_2 > 10$. Therefore, this

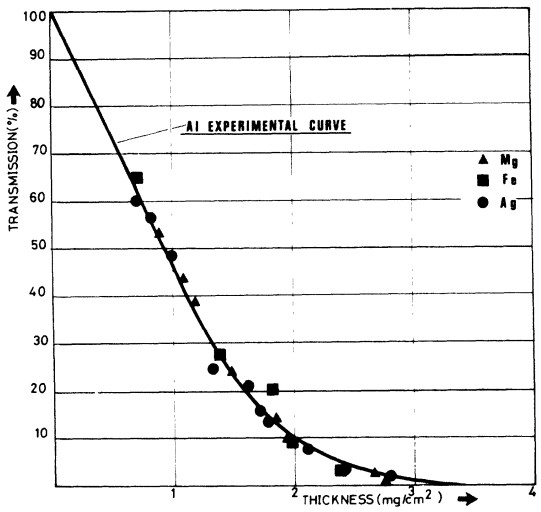

FIG. 3. Normalization of the experimental points to the transmission curve in Al.

formula is applicable to the results of the present experiment.

In fact, the fission fragments, as well as other ionizing particles, experience both electronic and nuclear stopping effects.

However, the nuclear stopping effect becomes significant only at low energy. For instance, as pointed out by Cumming and Crespo,[22] a fragment with $A_1 = 140$ and $Z_1 = 54$, when its energy is reduced to 17 MeV, feels a nuclear stopping which is only 10% of the total. Therefore, considering also that the final energy of the transmitted fission fragments must exceed the bias energy of the fission chamber,

TABLE I. Stopping powers relative to Al for U^{235} fission fragments and absolute range.

Element	Relative mass stopping power	Relative atomic stopping power	Absolute range (mg/cm²)	Absolute range (μ)
Mg	1.045 ± 0.030	0.941 ± 0.030	3.54	20.1
Al[a]	1	1	3.70	13.7
Fe	0.750 ± 0.045	1.552 ± 0.090	4.93	6.3
Ag	0.555 ± 0.010	2.222 ± 0.040	6.67	6.3

[a]Reference element.

it will be assumed that the stopping power for fission fragments is completely electronic. An experimental verification of this assumption can also be found in the work of Mulas and Axtmann,[15] who found the same quantitative results for stopping powers in H_2 and in D_2, at least for energies higher than 30 MeV.

A detailed comparison of the present experimental data with the LSS theory would be quite complicated due to the energy and atomic-number distributions of the fission fragments. However, a quite direct comparison is possible, which gives information on the validity of Eq. (3) in describing the Z_2 dependence of fission-fragment atomic stopping power.

Two kinds of fission fragments will be considered: a median light fission fragment ($A = 94.7$; $Z_1 = 37.4$; $E = 98.7$ MeV) and a median heavy fission fragment ($A = 138.8$; $Z_1 = 54.6$; $E = 67.5$ MeV).[36,37] Three theoretical curves and experimental values are shown in Fig. 4. The first two represent the atomic stopping power $(-1/N)\,dE/dX$ relative to Al as a function of Z_2 for the light and

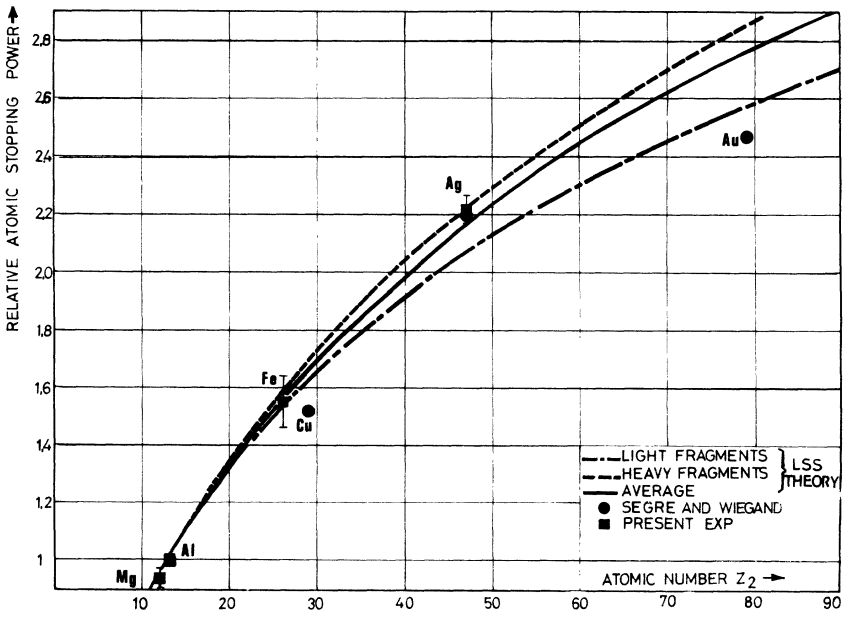

FIG. 4. Atomic stopping powers relative to Al as functions of the atomic number Z_2 of the stopping element.

the heavy fission fragments, respectively.

The curves obtained from Eq. (3) are of the form

$$S_{Al}(Z_2)=\frac{Z_2}{(Z_1^{2/3}+Z_2^{2/3})^{3/2}}\Big/\frac{Z_{Al}}{(Z_1^{2/3}+Z_{Al}^{2/3})^{3/2}}\ , \quad (4)$$

with Z_1 assuming the value of the light fragment ($Z_l = 37.4$) and the value of the heavy fragment ($Z_h = 54.6$), respectively.

The third theoretical curve shown in Fig. 4 represents the average of the light fragment and the heavy fragment. It is obtained by using the equation derived in Appendix C:

$$\bar{S}_{Al}(Z_2)=\frac{Z_l^{1/6}[Z_l Z_2/(Z_l^{2/3}+Z_2^{2/3})^{3/2}][\int_{E_l}^{0}(v_0/v)\,dE]^{-1}+Z_h^{1/6}[Z_h Z_2/(Z_h^{2/3}+Z_2^{2/3})^{3/2}][\int_{E_h}^{0}(v_0/v)\,dE]^{-1}}{Z_l^{1/6}[Z_l Z_{Al}/(Z_l^{2/3}+Z_{Al}^{2/3})^{3/2}][\int_{E_l}^{0}(v_0/v)\,dE]^{-1}+Z_h^{1/6}[Z_h Z_{Al}/(Z_h^{2/3}+Z_{Al}^{2/3})^{3/2}][\int_{E_h}^{0}(v_0/v)\,dE]^{-1}}\ . \quad (5)$$

In Eq. (5) the two sets of data reported above were used.

From the comparison with the experimental data, it appears that all three curves are in satisfactory agreement with the results of the present experiment. In particular, one must emphasize the agreement of the present data for Ag with the data of Segrè and Wiegand and of both with the theoretical value. We believe this fact would remove the reservations made by Segrè and Wiegand concerning the reliability of the measurements on this element, due mainly to the discrepancy between the Ag data and the theoretical dependence they assumed for the stopping power on Z_2,

$$S = a Z_2^{1/2}\ , \quad (6)$$

a being a suitable constant.

On the other hand, the value for the stopping power for Au, obtained by Segrè and Wiegand, which was in good agreement with Eq. (6), appears to be somewhat lower than predicted by Eqs. (4) and (5). It would be interesting to add new data to those already existing in order to obtain evidence for an eventual oscillatory behavior of the dependence of the average stopping power on Z_2.

Concerning the range values reported in Table I, it must be stressed that they are based on the value of 3.7 mg/cm^2 obtained by Segrè and Wiegand for the absolute range of U^{235} fission fragments in Al.

The ranges for the other elements are obtained by combining this value with the mass stopping power relative to the Al. This procedure is justified if it is assumed, as discussed in the preceding section, that the measured relative stopping powers are independent of the counter bias energy E_b. Obviously, the accuracy in the given ranges depends on the accuracy in the absolute value for Al.

In conclusion it can be stated that the experimental data reported here on the relative atomic stopping powers for U^{235} fission fragments are in good agreement with the LSS theory.

ACKNOWLEDGMENTS

Thanks are due to the staff of the RB-2 reactor and to Dr. T. DeLillo for agreeable collaboration, and to Dr. W. Kley and Dr. D. Marx for useful discussions. Thanks are also due to Professor J. Lindhard for kindly sending us several of his own publications on the subject.

APPENDIX A: TRANSMISSION OF FISSION FRAGMENTS THROUGH FOIL OF STOPPING ELEMENT

An expression for the transmission of fission fragments through the foil of stopping element will be derived based on a similar derivation in Ref. 36. It is assumed that the fission fragments are produced in the layer of uranium of zero thickness (Fig. 5) with an isotropic angular distribution.[36]

Let us consider first the transmission through the thickness x of the stopping element Z_2 of a fission fragment of atomic number Z_i and energy E having a range $R(Z_i, Z_2, E)$. The transmitted percentage as compared to thickness 0 is given by

$$T(x) = (1/2\pi)\int_0^{\theta(x)} 2\pi \sin\theta\, d\theta\ , \quad (A1)$$

where

$$\cos\theta(x) = x/R(Z_i, Z_2, E)\ . \quad (A2)$$

By integrating, one obtains

$$T(x) = 1 - x/R(Z_i, Z_2, E)\ . \quad (A3)$$

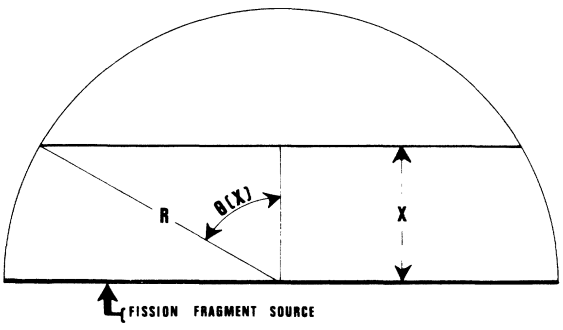

FIG. 5. Geometry of fission-fragment escape.

If $n(Z_i, E)$ is the atomic number and energy distribution of fission fragments, the theoretical transmitted fraction which would be measured in the present experiment if E_b were zero is given by

$$T_t(x) = \frac{\sum_i \int n(Z_i, E)[1 - x/R(Z_i, Z_2, E)]dE}{\sum_i \int n(Z_i, E)\,dE} \quad . \quad \text{(A4)}$$

Actually, as seen above, the measurements refer to an experimental range of the fission fragments $R_e(Z_1, Z_2, E, E_b)$ depending on the counter bias energy E_b. The actually measured transmission curves are then given by

$$T_e(x) = \frac{\sum_i \int n(Z_i, E)[1 - x/R(Z_i, Z_2, E, E_b)]dE}{\sum_i \int n(Z_i, E)\,dE} \quad . \quad \text{(A5)}$$

APPENDIX B: LACK OF DEPENDENCE OF RELATIVE STOPPING POWER ON BIAS ENERGY E_b

From Eqs. (2) and (3) the following expression is obtained for $R_e(Z_i, Z_2, E, E_b)$:

$$R_e(Z_i, Z_2, E, E_b) = \left[N\xi_e 8\pi e^2 a_0 \frac{Z_i Z_2}{(Z_i^{2/3} + Z_2^{2/3})^{3/2}} \right]^{-1} \times \int_E^{E_b} \frac{v_0}{v}\, dE \quad . \quad \text{(B1)}$$

If this expression is inserted into Eq. (A5), it is seen that by changing the value of E_b from E_{b1} to E_{b2} the curve $T_e(x)$ which would correspond to fragments of atomic number Z_i and energy E would not change for every value of Z_2 if the thickness x of material is multiplied by the factor

$$K = \frac{\int_E^{E_{b2}} (v_0/v)\,dE}{\int_E^{E_{b1}} (v_0/v)\,dE} \quad . \quad \text{(B2)}$$

It can be observed that the factor (B2) is independent of Z_2 and Z_i and depends only on the energy E of the fission fragment besides on E_{b1} and E_{b2}. In order to explain the experimental results obtained by Segrè and Wiegand concerning the variation only of the abscissa scale in the transmission curve by varying E_b, it must then be assumed that all the fission fragments act as if they all had the same initial average energy $\bar{E}$. This value of energy inserted into Eq. (B2) would give the multiplication factor of the abscissa scale. Although this assumption is not *a priori* completely justified, it can, however, be better accepted if it is considered that, in general, E_b is much lower than E.

APPENDIX C: DERIVATION OF RELATIVE STOPPING POWER AVERAGED BETWEEN LIGHT AND HEAVY FRAGMENTS

Equation (A5) can be used to derive an expression for an average value between the light and heavy fission-fragment relative stopping power.

By supposing two types of particles, i.e., a heavy fragment with range R_h and a light fragment with range R_l, Eq. (A5) becomes

$$T(x) = \tfrac{1}{2}(1 - x/R_l) + \tfrac{1}{2}(1 - x/R_h) \quad \text{(C1)}$$

or

$$T(x) = 1 - x/\langle R \rangle \quad , \quad \text{(C2)}$$

where $\langle R \rangle$ is defined by

$$1/\langle R \rangle = \tfrac{1}{2}(1/R_l + 1/R_h) \quad . \quad \text{(C3)}$$

By using Eq. (B1) and by assuming that the average atomic stopping power could be written as $\bar{S}(Z_l, Z_h, Z_2)S(\bar{E})$ (i.e., that it can be separated into Z and E dependences), Eq. (C3) becomes

$$[\bar{S}(Z_l, Z_h, Z_2)]\left[\int_{\bar{E}}^{0} \frac{v_0}{v}\, dE\right]^{-1} = \frac{1}{2}\left\{\left[N\xi_e 8\pi e^2 a_0 \frac{Z_l Z_2}{(Z_l^{2/3} + Z_2^{2/3})^{3/2}}\right]\left[\int_{E_l}^{0} \frac{v_0}{v}\, dE\right]^{-1} + \left[N\xi_e 8\pi e^2 a_0 \frac{Z_h Z_2}{(Z_h^{2/3} + Z_2^{2/3})^{3/2}}\right]\left[\int_{E_h}^{0} \frac{v_0}{v}\, dE\right]^{-1}\right\} \quad , \quad \text{(C4)}$$

where use has also been made of Eq. (1).

From Eq. (C4), by remembering that ξ_e is proportional to $Z_1^{1/6}$, one obtains the final equation for the average atomic stopping power relative to Al as a function of Z_2,

$$\bar{S}_{Al}(Z_2) = \frac{Z_l^{1/6}[Z_l Z_2/(Z_l^{2/3} + Z_2^{2/3})^{3/2}]\left[\int_{E_l}^{0}(v_0/v)\,dE\right]^{-1} + Z_h^{1/6}[Z_h Z_2/(Z_h^{2/3} + Z_2^{2/3})^{3/2}]\left[\int_{E_h}^{0}(v_0/v)dE\right]^{-1}}{Z_l^{1/6}[Z_h Z_{Al}/(Z_l^{2/3} + Z_{Al}^{2/3})^{3/2}]\left[\int_{E_l}^{0}(v_0/v)\,dE\right]^{-1} + Z_h^{1/6}[Z_h Z_{Al}/(Z_h^{2/3} + Z_{Al}^{2/3})^{3/2}]\left[\int_{E_h}^{0}(v_0/v)dE\right]^{-1}} \quad . \quad \text{(C5)}$$

---

*On leave from Bologna University.

†Present address: Institut Max von Laue-Paul Langevin, Grenoble, France.

[1] J. Lindhard, M. Scharff, and H. E. Schiøtt, Kgl. Danske Videnskab. Selskab, Mat.-Fys. Medd. 33, No. 14 (1963).

[2] R. L. Wolke, W. N. Bishop, E. Eichler, N. R. Johnson, and G. D. O'Kelley, Phys. Rev. 129, 2591 (1963).

[3] P. Zahn, Z. Physik 172, 85 (1963).

[4] S. K. Allison, D. Auton, and R. A. Morrison, Phys. Rev. 138, A688 (1965).

[5]J. T. Park, Phys. Rev. 138, A1317 (1965).
[6]C. A. Sautter and E. J. Zimmermann, Phys. Rev. 140, A490 (1965).
[7]P. Dahl and J. Magyar, Phys. Rev. 140, A1420 (1965).
[8]C. Chasman, K. W. Jones, and R. A. Ristinen, Phys. Rev. Letters 15, 245 (1965).
[9]J. H. Ormrod, J. R. Macdonald, and H. E. Duckworth, Can. J. Phys. 43, 275 (1965).
[10]R. D. Moorhead, J. Appl. Phys. 36, 391 (1965).
[11]P. H. Barker and W. R. Phillips, Proc. Phys. Soc. (London) 86, 379 (1965).
[12]N. K. Aras, M. P. Menon, and G. E. Gordon, Nucl. Phys. 69, 337 (1965).
[13]V. Subrahmanyan and M. Kaplan, Phys. Rev. 142, 174 (1966).
[14]M. Kaplan and J. L. Richards, Phys. Rev. 145, 153 (1966).
[15]P. M. Mulas and R. C. Axtmann, Phys. Rev. 146, 296 (1966).
[16]V. A. J. Van Lint, M. E. Wyatt, R. A. Schmitt, C. S. Suffredini, and D. K. Nichols, Phys. Rev. 147, 242 (1966).
[17]C. D. Moak and M. D. Brown, Phys. Rev. 149, 244 (1966).
[18]G. B. Saha and N. T. Porile, Phys. Rev. 151, 907 (1966).
[19]D. Marx, Z. Physik 195, 26 (1966).
[20]C. Chasman, K. W. Jones, R. A. Ristinen, and J. T. Sample, Phys. Rev. 154, 239 (1967).
[21]L. B. Bridwell, L. C. Northcliffe, S. Datz, C. D. Moak, and H. O. Lutz, Phys. Rev. 159, 276 (1967).
[22]J. B. Cumming and V. P. Crespo, Phys. Rev. 161, 287 (1967).
[23]T. E. Pierce, W. W. Bowman, and M. Blann, Phys. Rev. 172, 287 (1968).
[24]T. E. Pierce and M. Blann, Phys. Rev. 173, 390 (1968).
[25]A. H. El Hoshy and J. F. Gibbons, Phys. Rev. 173, 454 (1968).
[26]W. K. Chu, P. D. Bourland, K. H. Wang, and D. Powers, Phys. Rev. 175, 342 (1968).
[27]N. T. Porile and I. Fujiwara, Phys. Rev. 176, 1166 (1968).
[28]R. Kalish, L. Grodzins, F. Chmara, and P. H. Rose, Phys. Rev. 183, 431 (1969).
[29]W. K. Chu and D. Powers, Phys. Rev. 187, 478 (1969).
[30]W. White and R. M. Mueller, Phys. Rev. 187, 499 (1969).
[31]B. Chinaglia, F. DeMichelis, and A. Tartaglia, Nuovo Cimento Letters 4, 1185 (1970).
[32]E. Segrè and C. Wiegand, Phys. Rev. 70, 808 (1946).
[33]G. Maracci, F. Rustichelli, V. Aiello, and T. De Lillo, Nucl. Instr. Methods 62, 57 (1968).
[34]F. Rutichelli and G. Maracci, Euratom Report No. 4326i, 1969 (unpublished).
[35]L. C. Northcliffe, Ann. Rev. Nucl. Sci. 13, 67 (1963).
[36]J. M. Alexander and M. F. Gadzik, Phys. Rev. 120, 874 (1960).
[37]M. S. Moore and L. G. Miller, Phys. Rev. 157, 1049 (1967).

PHYSICAL REVIEW B VOLUME 4, NUMBER 11 1 DECEMBER 1971

Microscopic Analysis of Exchange and Motional Narrowing

J. P. Boucher
Laboratoire de Résonance Magnétique, Centre d'Etudes Nucléaires de Grenoble, Cedex 85, 38 *Grenoble-Gare, France*
(Received 12 July 1971)

From a microscopic analysis of the paramagnetic resonance line, the exchange- and motional-narrowing phenomena are shown to be basically distinct. Exchange-narrowed lines are essentially made up of the Fourier transform of the cross-correlation functions; motional-narrowed lines are only formed by the Fourier transform of the self-correlation function.

In this paper, we wish to discuss the well-known phenomenon of the narrowing of paramagnetic resonance lines. This effect is caused by the exchange interactions between spins in solids or by the motions of the atoms or molecules which carry the spin in liquids. Usually, the theory is investigated from a macroscopic treatment of the correlation function, whose frequency Fourier transform gives the spectral resonance line. The most complete theory had been given by Kubo and Tomita.[1] These authors use a perturbation expansion, and in one general formalism they can explain both the exchange and the motional narrowing. The mathematical property which leads to this result is the fact that the Hamiltonian operators of the exchange or motional interactions, E and M, respectively, commute with the components $\alpha = x, y, z$ of the total spin

$$\vec{S} = \sum_i \vec{s}_i , \tag{1}$$

$\vec{s}_i$ being an individual spin:

$$\left[S^{\alpha}, \begin{Bmatrix} E \\ M \end{Bmatrix} \right] = 0 . \tag{2}$$

Thus, the understanding of these two phenomena is apparently quite the same. The exchange in solids causes rapid motion in the spin system, which produces an averaging out of the effects of the broad-